# *SUZAKU* OBSERVATION OF A HARD EXCESS IN 1H 0419−577: DETECTION OF A COMPTON-THICK PARTIAL-COVERING ABSORBER

T. J. Turner[1,2], L. Miller[3], S. B. Kraemer[2,4], J. N. Reeves[5], and K. A. Pounds[6]
[1] Department of Physics, University of Maryland Baltimore County, Baltimore, MD 21250, USA
[2] Astrophysics Science Division, NASA/GSFC, Greenbelt, MD 20771, USA
[3] Department of Physics, University of Oxford, Denys Wilkinson Building, Keble Road, Oxford OX1 3RH, UK
[4] Institute for Astrophysics and Computational Sciences, Department of Physics, The Catholic University of America, Washington, DC 20064, USA
[5] Astrophysics Group, School of Physical and Geographical Sciences, Keele University, Keele, Staffordshire ST5 5BG, UK
[6] Department of Physics and Astronomy, University of Leicester, Leicester LE1 7RH, UK

## ABSTRACT

We present results from a 200 ks *Suzaku* observation of 1H 0419−577 taken during 2007 July. The source shows a strong excess of counts above 10 keV compared to the extrapolation of models based on previous data in the 0.5–10 keV band. The "hard excess" in 1H 0419−577 can be explained by the presence of a Compton-thick partial-covering absorber that covers ∼70% of the source. The Compton-thick gas likely originates from a radius inside of the optical broad-line region and may form part of a clumpy disk wind. The fluorescent Fe Kα luminosity measured by *Suzaku* is consistent with that expected from an equatorial disk wind.

*Key words:* galaxies: active – galaxies: individual (1H 0419−577) – galaxies: Seyfert – X-rays: galaxies

*Online-only material:* color figures

## 1. INTRODUCTION

1H 0419−577 is a broad-line Seyfert 1 galaxy located at a redshift $z = 0.104$ (Grupe 1996; Thomas et al. 1998; Turner et al. 1999) with a strong ultraviolet (UV) flux (Marshall et al. 1995). The X-ray properties of this active galactic nucleus (AGN) have been the subject of much discussion, as the source shows a strong steepening to soft energies and marked spectral variability (Guainazzi et al. 1998; Turner et al. 1999; Page et al. 2002). The extreme nature of the spectral variability of this source is especially interesting since systematic flattening at low flux levels is a common property of Seyfert galaxies (e.g., Papadakis et al. 2002; Pounds et al. 2004a, 2004b; Vaughan & Fabian 2004; Miller et al. 2008; Turner et al. 2008). Understanding the origin of the observed phenomenon should lead to important insight as to the physical processes that dominate in such sources. The AGN low-state spectra have been suggested by some (e.g., Vaughan & Fabian 2004; Miniutti & Fabian 2004) to represent blurred reflection arising within $20r_g$ and by others to represent a complex absorbed state (e.g., Inoue & Matsumoto 2003; Pounds et al. 2003; Miller et al. 2008). In the context of the former model, spectral variability has been attributed to changes in the degree of light bending as the continuum source location moves; for absorption-based models spectral variability is attributed to changes in the ionization, column or covering of absorbing gas (e.g., Netzer et al. 2002; Kraemer et al. 2005). As for many sources, detailed models for 1H 0419−577 have been suggested whereby the spectral form and variability can be explained either by a partial-covering absorber (Pounds et al. 2004a, 2004b) or blurred reflection from the inner accretion disk (Fabian et al. 2005); data prior to *Suzaku* were unable to provide a definitive preference for either of the two scenarios.

Recent improvements in the quality of data available in the Fe K regime has led to the detection in AGN of relatively narrow absorption lines of high equivalent width (greater than 50 eV, e.g., Pounds et al. 2003; Miller et al. 2007; Dadina et al. 2005; Braito et al. 2007; Turner et al. 2008), indicative of an origin in very large columns of ionized gas. Narrow absorption

lines cannot arise from blurred reflection so their detection motivates a reconsideration of the importance of absorption in shaping the observed X-ray properties of AGN. This and the extended bandpass afforded by the combination of X-ray Imaging Spectrometer (XIS) and positive-intrinsic-negative (PIN) data motivated a *Suzaku* observation of 1H 0419−577 that is the subject of this paper.

## 2. OBSERVATIONS

*Suzaku* (Mitsuda et al. 2007) has four X-ray telescopes each focusing X-rays on to a CCD forming part of the XIS (Koyama et al. 2007) suite. XIS units 0, 2, and 3 are front illuminated (FI) and cover ∼0.6–10.0 keV with energy resolution FWHM ∼150 eV at 6 keV. Use of XIS2 was discontinued after a charge leak was discovered in 2006 November. XIS1 is a back-illuminated CCD and has an enhanced soft-band response (down to 0.2 keV) but lower area at 6 keV than the FI CCDs as well as a larger background level at high energies. *Suzaku* also carries a nonimaging, collimated Hard X-ray Detector (HXD; Takahashi et al. 2007) whose PIN detector provides useful AGN data typically over 15–70 keV.

The *Suzaku* observation was made 2007 July 25 (OBSID 702041010). We reran the pipeline processing of the raw data to utilize the most recent calibration with hxdpi and hxdgrade versions 2008 March 3. The data were then reduced using v6.4.1 of HEAsoft. We screened the events to exclude data during and within 500 s of entry/exit from the South Atlantic Anomaly (SAA). Additionally, we excluded data with an Earth elevation angle less than $10°$ and cutoff rigidity $> 6$ GeV. The source was observed at the nominal center position for the XIS. The FI CCDs were in $3 \times 3$ and $5 \times 5$ edit modes, with normal clocking mode. For the CCDs utilized, we selected good events with grades 0, 2, 3, 4, and 6 and removed hot and flickering pixels using the SISCLEAN script. The spaced-row charge injection (SCI) was utilized. The exposure time was 179 ks for the FI CCDs.

The XIS products were extracted from circular regions of 2′.9 radius while background spectra were extracted from a

region of the same size offset from the source (and avoiding the chip corners where calibration source data are registered). The response and ancillary response files were then created using xisrmfgen v2007 May and xissimarfgen v2008 Mar. The background was 1% of the total XIS count rate in the full XIS band for each CCD.

1H 0419−577 is too faint to be detected in the HXD GSO instrument, but was detectable in the PIN. For the analysis we used the model "D" background (released 2008 June 17[7]). As the PIN background rate is strongly variable around the orbit, we first selected source data to discard events within 500 s of an SAA passage, we also rejected events with day/ night elevation angles >5°. The time filter resulting from the screening was then applied to the background events model file to give PIN model-background data for the same time intervals covered by the on-source data. The net exposure time was 142 ks. As the background events file was generated using 10 times the actual background count rate, an adjustment to the background spectrum was applied to account for this factor. hxddtcor v2007 May was run to apply the deadtime correction to the source spectrum. To take into account the cosmic X-ray background (Boldt & Leiter 1987; Gruber et al. 1999) xspec v 11.3.2ag was used to generate a spectrum from a cosmic X-ray background (CXB) model (Gruber et al. 1999) normalized to the 34′ × 34′ Suzaku PIN field of view, and combined with the PIN instrument background file to create a total background file. The flux of the CXB component is $8 \times 10^{-12}$ erg cm$^{-2}$ s$^{-1}$ in the 15–50 keV band. The source comprised 15% of the total counts in the PIN band. We used the response file ae_hxd_pinxinome3_20080129.rsp for spectral fitting.

Spectral fits utilized data from the XIS instrument, detectors 0 and 3, in the energy range 0.6–10 keV and also from the PIN instrument providing useful data in the energy range 15–50 keV for this weak source. XIS1 was not used owing to the higher background level at high energies. In the spectral analysis, the pin flux was increased by a factor 1.16 which is the appropriate adjustment for the instrument cross-calibration at the epoch of the observation.[8] Data in the range 1.78–1.9 keV were excluded from the XIS due to uncertainties in calibration around the instrumental Si K edge. A 2% systematic error was applied to the PIN background spectrum before spectral fitting. XIS data were binned at the half-width at half-maximum resolution for each instrument, optimal for detection of spectral features while PIN data were binned to be a minimum of 5σ above the background level for the spectral fitting.

## 3. SPECTRAL FITTING RESULTS

### 3.1. Initial Results

During our Suzaku observation, the source was found to have (background subtracted) count rates 2.613 ± 0.004 (summed XIS0,3) and (5.42 ± 0.17) × 10$^{-2}$ (PIN) count s$^{-1}$ corresponding to a 2–10 keV source flux $1.8 \times 10^{-11}$ erg cm$^{-2}$ s$^{-1}$ and 0.5– 2 keV flux $1.4 \times 10^{-11}$ erg cm$^{-2}$ s$^{-1}$. These fluxes represent a high state as compared to the ranges 0.9–1.6 × 10$^{-11}$ erg cm$^{-2}$ s$^{-1}$ in the 2–10 keV band (Pounds et al. 2004a; Page et al. 2002) and (0.2–1.3) × 10$^{-11}$ erg cm$^{-2}$ s$^{-1}$ in the 0.5– 2 keV band observed by XMM.

The full-band XIS light curve showed only modest variability of ±40% around the mean. The PIN-band flux did not show
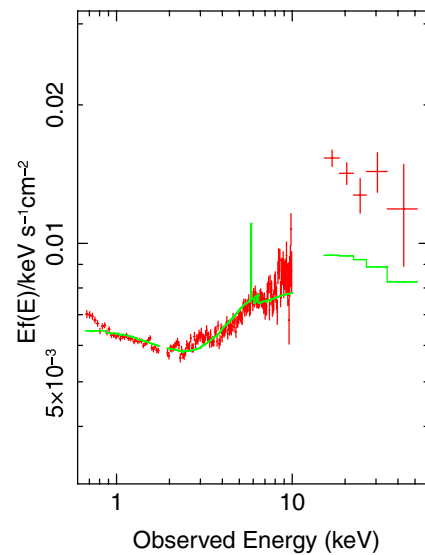
**Figure 1.** Suzaku XIS0 + 3 and PIN data (red) compared to the XMM-based absorption model (solid green line). PIN data are rebinned more than 5σ above the background for the plot only.

(A color version of this figure is available in the online journal.)

any significant variability within the observation. The weakness of the target combined with the relatively low level of flux variability meant that it was not possible to extract a useful decomposition of the data using principal components analysis (Miller et al. 2007). Thus, in this paper we report only upon analysis of the mean Suzaku spectrum and application of our model to the older XMM spectra.

Pounds et al. (2004a, 2004b) developed an absorption-based model for 1H 0419−577 where variations in the opacity or covering fraction of the absorber could explain the marked spectral variability correlated with flux; that model had one partial-covering absorber and one full screen of gas intrinsic to the AGN. We constructed a model of that form and a fit was performed allowing the power-law index, normalization, column densities, and ionization states all to be free. The model also included a full-covering screen of neutral gas fixed at the Galactic line-of-sight column and the emission features detected by the XMM Reflection Grating Spectrometers (Pounds et al. 2004b) that fell within our bandpass. As shown in Table 1 (row 1), this fit yielded $\chi^2 = 631/188$ degrees of freedom (dof). The model is unable to account for the excess of counts above 10 keV (Figure 1), where data lie more than ∼50% above the expected flux.

Before fitting models in more detail, we performed some additional analysis. As the background level dominates the PIN count rate, we focus on the reliability of the new PIN background model to determine the robustness of the PIN result. We reprocessed the PIN data using the old background model ("A") and old processing pipeline. This combination yields a background-subtracted flux for 1H 0419−577 that is 8% lower than that for the new processing with new model D background. Refitting the data using the older version of the PIN pipeline and background model reduces the PIN excess by 10% but still leaves a highly significant excess. Unfortunately, there were no Earth occultation data to test against the PIN model predicted rates for this date and time of observation. To check whether thermal noise in the PIN detector might affect the PIN rate, which can sometimes be a problem below 20 keV, we conservatively rescreened the PIN data to discard events

**Table 1**
Partial-Covering Model

| $\Gamma$ | $N_H1$ [a] | $\log \xi1$ | $C1$ [b] | $N_H2$ [a] | $\log \xi2$ | $C2$ [b] | $\chi^2/\text{dof}$ |
|---|---|---|---|---|---|---|---|
| 2.19 | 0.66 | −3.0 | 48% | 0.03 | 4.1 | 100% | 631/188 |
| $2.31 \pm 0.04$ | $0.54^{+0.11}_{-0.21}$ | $-0.13^{+0.80}_{-1.09}$ | $16 \pm 3\%$ | $18.5^{+1.9}_{-3.7}$ | $1.90^{+0.16}_{-0.49}$ | $66^{+12}_{-3}\%$ | 260/187 |

**Notes.** A column of neutral gas covered all components, fixed at the Galactic value $2.0 \times 10^{20}$ cm$^{-2}$.
Errors are calculated at 90% confidence but only shown for the best fit.
[a] Column density in units of $10^{23}$ atom cm$^{-2}$.
[b] Percentage covering.

within 5760 s of an SAA passage. No significant difference was found between the more tightly screened PIN spectrum and the nominally processed version so there seems to be no thermal problem with the few PIN channels used below 20 keV. Finally, as the $1\sigma$ uncertainty on the model D background is 1.3%, we increased the PIN background spectrum by $3\sigma$ and found this did not significantly reduce the PIN hard excess. The tests performed indicate that the PIN result for this AGN is robust to the precise method of PIN background estimation used.

The PIN field of view is $34' \times 34'$ and as this is not an imaging instrument we checked sky catalogs and confirmed that no known hard X-ray sources lie within the PIN field of view that could contaminate our spectrum. The *ASCA* GIS images are particularly useful as these cover 0.7–10.0 keV with a field of view $50'$ diameter. *ASCA* GIS images[9] taken 1996 July and August show that there are no other hard X-ray sources detected in the field of view at that epoch.

H 0419−577 was detected in the Burst Array Telescope (BAT) survey (Tueller et al. 2008). The BAT spectrum was downloaded from the public archive[10] and fitted with our model to determine the flux in a bandpass that can be compared directly to the 2007 PIN data. We found a mean BAT flux for the period 2005 December – 2006 September $F_{15-50} = 1.5^{+0.38}_{-0.36} \times 10^{-11}$ erg cm$^{-2}$ s$^{-1}$, lower than the PIN flux over the same band $F_{15-50} = (2.6 \pm 0.13) \times 10^{-11}$ erg cm$^{-2}$ s$^{-1}$. Another hard-band measurement was obtained using the *BeppoSAX* PDS which gave $F_{15-136} = (1.2 \pm 0.56) \times 10^{-11}$ erg cm$^{-2}$ s$^{-1}$ (Deluit & Courvoisier 2003) compared to the extrapolation of the PIN fit which yields $F_{15-136} = 3.5 \pm 0.2 \times 10^{-11}$ erg cm$^{-2}$ s$^{-1}$. In conclusion, comparison of measurements above 10 keV shows some evidence for flux variability and we return to this point in Section 4.

### 3.2. Fitting Absorption-Dominated Models

In the context of absorption models, the hard excess is indicative of the presence of a layer of Compton-thick gas partially covering the continuum source. (The continuum optical depth has a value of unity for $N_H \simeq 1/1.2\sigma_T \simeq 1.25 \times 10^{24}$ cm$^{-2}$ and so we refer to a column of gas at or above this threshold as Compton thick). To fit the PIN data, we modified the Pounds et al. (2004a, 2004b) model to allow the second absorber to have a covering fraction less than 1, and have a different column density and ionization state to that previously fitted.

Initially, we used a table generated from XSTAR v21ln8 with gas density assumed to be $n = 10^{10}$ cm$^{-3}$, an illuminating spectrum comprising a power law of index $\Gamma = 2.3$ and a gas turbulent velocity 300 km s$^{-1}$. The value of assumed turbulent velocity is of great importance when one is deriving ionic column densities from fitting narrow absorption lines

and varying the turbulent velocity over the range 100–500 km s$^{-1}$ can lead to changes in the inferred column density by an order of magnitude (e.g., Young et al. 2005). However, the absorber fits here are based upon detection of broad features and overall spectral curvature and so are not very sensitive to turbulent velocity assumed in generating the table. The fit is shown in Table 1 (errors are only given on the best fit). A limitation of XSTAR is that spectral modification from Compton scattering or "Comptonization," important for Compton-thick gas, is neglected: in our solution, one zone of gas falls at a value where these effects start to become important and so our model for the source is, in that sense, an approximation to the true physical situation. However, as our fit falls so close to the Compton-thick boundary, and as many assumptions have had to be made in the fitting, we consider this an adequate parameterization for data of this quality.

The power-law continuum has three sight lines, 18% of the continuum is absorbed only by the Galactic column, 66% of the observed continuum has passed through a Compton-thick column, and 16% through $\sim 5 \times 10^{22}$ cm$^{-2}$ (that we dub the "intermediate layer") and the fit is shown in Figure 2. The model was constructed and parameters tabulated for a physical interpretation where two partial-covering absorbers are cospatial. Obviously, different interpretations of the fit can be made if the gas layers are assumed to lie one inside of the other; an obvious possibility is that the intermediate layer lies outside of the Compton-thick clouds (constructing the model in that way does not significantly change the fitted $\xi$ and $N_H$ values but changes the inferred covering fraction for the intermediate layer to 82%). In Section 4, we assume the former, cospatial, geometry.

The solution we have found for the Compton-thick zone (Table 1) leads to an expectation of weak absorption lines from Fe in the 6.4–6.6 keV regime. However, owing to the low covering fraction of the gas the equivalent width of the strongest absorption line would be $<10$ eV, undetectable in these data.

The Fe K$\alpha$ line was found to have a peak energy $6.39 \pm 0.06$ keV, $\sigma = 0.07^{+0.33}_{-0.07}$ keV, $n = 6.2^{+6.6}_{-2.2} \times 10^{-6}$ photons cm$^{-2}$ s$^{-1}$ yielding an equivalent width 30 eV against the total observed continuum. The combined uncertainties in line width and flux leave this measurement consistent with those from *XMM* data (Pounds et al. 2004a, 2004b). The column density returned from the fit is degenerate with $\xi$ and depends on the gas density assumed in the XSTAR model run; consequently the XSTAR table density significantly affects the estimate of flux lost to scattering in the Compton-thick gas. Fitting the data using a model table with $n = 10^{12}$ cm$^{-3}$, the column density for the highest column layer fell to $9.7^{+0.64}_{-0.48} \times 10^{23}$ cm$^{-2}$ with $\log \xi = 0.82^{+0.14}_{-0.21}$.

The dominant remaining contribution to $\chi^2$ is at 1.55 keV (Figure 3), coincident with the Al detector edge. While the Al edge is much weaker than the Si edge (whose peak energy band
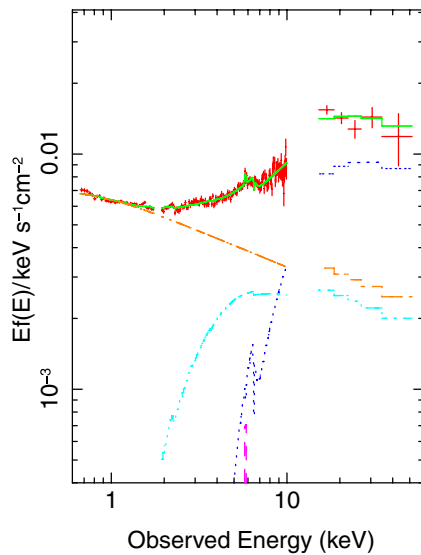
**Figure 2.** *Suzaku* XIS0 + 3 and PIN data (red) compared to the best partial-covering model. The solid (green) line represents the sum of all model components, the dotted (orange) line represents the uncovered fraction of the continuum, the dashed (dark blue) line is the fraction of continuum absorbed by Compton-thick gas, the dot-dashed (aqua) line is the fraction of continuum under $5 \times 10^{22}$ cm$^{-2}$, and the dashed (purple) line is the Fe K$\alpha$ emission.
(A color version of this figure is available in the online journal.)

is excluded from the fit), the presence of a detector feature at an energy where we see an isolated emission line of uncertain identification is problematic, and thus we do not attempt to assign an astrophysical explanation to the feature.

We also tried a variation on this model that included a component of (unblurred) reflection linked to the Fe K line by a factor 725 in normalization and parameterized by the XSPEC model PEXRAV; this linked component pair physically represents reflection from distant neutral material illuminated by a continuum of slope $\Gamma = 2.3$ (with a high-energy cutoff outside of the PIN bandpass) for a disk inclined at $\theta = 60°$ to the observer's line of sight (George & Fabian 1991). However, in the fitting process we found this PEXRAV component to be sufficiently weak that its inclusion did not improve the fit or significantly affect the absorption parameters.

The flux observed for 1H 0419−577 during the *Suzaku* observation corresponds to an observed luminosity $L_{2-10} = 4.2 \times 10^{44}$ erg s$^{-1}$, (assuming $H_0 = 75$ km s$^{-1}$ Mpc$^{-1}$ throughout this paper). The absorption-corrected flux and luminosity are $F_{2-10} = 5.3 \times 10^{-11}$ erg cm$^{-2}$ s$^{-1}$, $L_{2-10} = 1.3 \times 10^{45}$ erg s$^{-1}$ (with no significant difference between the fits using tables of different density gas). We also need to account for the scattering losses in the high-column gas zones. For the first solution (Table 1) assuming that the filling factor of the gas is low (such that no significant flux is scattered back into the line of sight) then, as the column $1.85 \times 10^{24}$ cm$^{-2}$ transmits only 29% of the incident flux, a factor 3.4 correction must be applied to the fraction of flux observed through that layer to estimate the total true intrinsic luminosity. For the alternative model solution, yielding $9.7 \times 10^{23}$ cm$^{-2}$, the scattered flux is half of that incident on the cloud, under the same assumption about filling. Correcting the fraction of flux coming through the Compton-thick zone for scattering losses, we thus estimate that the intrinsic luminosity for the source must lie in the range $L_{2-10} \sim (2-3) \times 10^{45}$ erg s$^{-1}$ and from these values the bolometric luminosity is estimated (Elvis et al. 1994) to be $L_{bol} \sim (7-11) \times 10^{46}$ erg s$^{-1}$.
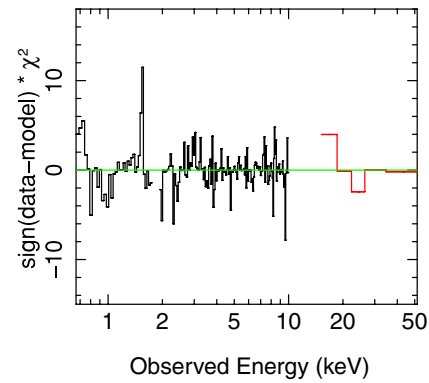


**Figure 3.** $\chi^2$ residuals to the best X-ray fit shown in Figure 2, from fitting a partial-covering model as detailed in Table 1.
(A color version of this figure is available in the online journal.)

Finally, there is an intriguing possibility that the underlying continuum is curved, as evidenced by examination of the difference spectrum from *XMM* data (Pounds et al. 2004b). As we have not sampled a large range of flux in this *Suzaku* observation, we are unable to test this idea further but note that a simple extrapolation of the Comptonized spectral form found by Pounds et al. (2004b) into the PIN band would increase the implied hard excess.

### 3.3. Extension to XMM High/Low Data

As reported by Page et al. (2002) and Pounds et al. (2004a, 2004b), the 2000 December (OBSID 0112600401) and 2002 September (OBSID 0148000201) *XMM* observations of 1H 0419−577 sampled the source across a wide range of flux states, ideal for testing the applicability of the *Suzaku* model to other epochs. We reduced the *XMM* data following the method and using the criteria of Pounds et al. (2004b) except that SAS version 8.0.0 was utilized and only the pn data were extracted. We fitted the spectra fixing the photon index, column densities, and ionization states of the two absorbing layers from the *Suzaku* fit using the $n = 10^{10}$ cm$^{-3}$ case as in Table 1. Assuming a model construction as before, we found the high state to yield a solution whereby 18% ± 1% of the source is uncovered, 24% ± 2% is covered by the intermediate layer of $\sim 5 \times 10^{22}$ cm$^{-2}$, and $58^{+21}_{-14}$% also lies under the Compton-thick absorber. Fitting the *XMM* low-state data, we found that only 3% ±1% of the flux was unobscured, while 27% ± 4% was covered by the intermediate column and 70% ± 16% also covered by the Compton-thick layer. As found for several other sources, and previously suggested for 1H 0419−577 (Pounds et al. 2004b), the dominant change in spectral shape observed below 10 keV is consistent with changes in the fraction of unobscured continuum, while all data are consistent with the same column density and ionization state for the gas. Noting that the energetically dominant hard band is much less variable than the soft-band X-rays, we examined the absorption- and scattering-corrected fluxes for the low- and high-state data and found that under the *Suzaku* model, both *XMM* data sets returned the same implied intrinsic continuum flux of $F_{2-10} \sim 5.4 \times 10^{-11}$ erg cm$^{-2}$ s$^{-1}$ showing the continuum source to be consistent with no intrinsic continuum variation between *XMM* epochs and thus attributing observed variations to changes in the absorbers. However, the issue of whether the continuum source is intrinsically constant remains unresolved: after both absorption and scattering corrections have been applied the *Suzaku* data imply an intrinsic continuum flux

$F_{2-10} \sim (8-15) \times 10^{-11}$ erg cm$^{-2}$ s$^{-1}$, higher than the *XMM* values.

### 3.4. Fitting Blurred Reflection Models

The *XMM* data for 1H 0419−577 have also previously been fitted successfully using a composite disk model (Fabian et al. 2005) with relativistic blurring parameterized by the XSPEC model KDBLUR (Laor 1991). The blurred model is constructed from the sum of a power law and reflection of that continuum from an ionized disk (Ross & Fabian 2005). To fit the *XMM* spectrum, Fabian et al. (2005) utilized a composite disk, i.e., one constructed to allow a change in the illumination pattern at a break radius, while the ionized absorbing gas was parameterized by an edge at 0.74 keV.

We fitted the data using a model with disk inclination, inner and outer radii, break radius, emissivity indices, and Fe abundance fixed at the values found by Fabian et al. (2005), as these parameters are not expected to vary with epoch or source flux. The normalization of the composite disk and of the power law, $\Gamma$, the ionization parameters and the absorption edge parameters were all allowed to be free. The model was fitted to the XIS and PIN data and yielded $\chi^2 = 1154/199$ dof), failing to fit the high PIN flux above 10 keV. We then freed the break radius and both emissivity indices, yielding $\chi^2 = 529/189$ dof with the fit again failing to explain the source flux above 10 keV. Further freeing the Fe abundance, disk inclination angle, inner radius and adding a narrow Fe emission line component yielded $\chi^2 = 337/183$ dof. Replacement of the absorption edge with a full screen of ionized absorbing gas did not yield a significant improvement. As the blurred reflection model does not fit the data, we continue with a discussion of the source in the context of the absorption-dominated model.

## 4. DISCUSSION

### 4.1. The Location of the Absorbing Zones

Data from several wave bands support the existence of partial-covering absorbers in AGN. UV spectroscopy reveals multiple zones of gas distinguished by different ionization states, covering fractions and kinematics. Partial covering by neutral gas and/or ionized absorbing gas has long been suggested as one possible way to explain the spectral curvature in AGN (e.g., Reichert et al. 1985; Holt et al. 1980) and the gas was found to be consistent with an origin in the optical broad-line region (BLR; Holt et al. 1980; Piro et al. 1992). Recent results from X-ray grating spectroscopy have shown that multiple layers of gas contribute to X-ray absorption, including columns of gas with $N_H \sim 10^{23}$–$10^{24}$ atoms cm$^{-2}$ with very high ionization states revealed by their H-like and He-like Fe K absorption lines (e.g., Young et al. 2005; Miller et al. 2007; Turner et al. 2008). In the context of absorption-dominated models, spectral variability is often explained by changes in covering or opacity of the gas layers, or a response in gas ionization state as the continuum varies (e.g., Netzer et al. 2002; Kraemer et al. 2005). Deep minima in the light curves of MCG-6-30-15 (McKernan & Yaqoob 1998) and NGC 3516 (Turner et al. 2008) support a variable-covering absorption picture as their dip profiles suggest an origin as eclipse events. Further support for the importance of absorption is seen from the short-timescale absorption line variations detected in NGC 1365 (Risaliti et al. 2005).

With the relatively low spectral resolution available in the X-ray regime to date, progress has been limited by the ambiguity between absorption and blurred reflection signatures: even the brightest and best studied AGN such as MCG-6-30-15 can be described using either model. (e.g., Miniutti et al. 2003, 2007; Miniutti & Fabian 2004; Inoue & Matsumoto 2003; Miller et al. 2008). However, the break to a hard excess in the *Suzaku* PIN data for 1H 0419−577 is sufficiently sharp that a preference is found for a partial-covering model: the Compton-thick zone covers 66% of the continuum source, similar to the covering fractions implied for several other high-column partial-covering absorbers (e.g., Reeves et al. 2002, 2003; Miller et al. 2007; Turner et al. 2007).

A common argument against partial-covering models is based on probability, i.e., that to have a covering fraction such as ∼70% with significant observed variations in covering (here of order 10% between flux states) implies that there must be obscuration from a few clouds subtending a similar transverse size on the sky as the continuum source. Obviously, if the clouds exist as far out as the BLR then the probability of observing an orbiting cloud cross the line of sight is low. However, the distances estimated for absorbing clouds depend on the cloud density assumed. If one assumes a high density for the absorber (e.g., $n \gtrsim 10^{12}$ cm$^{-2}$) then the material is indicative of an origin close to the active nucleus and the probability issue is alleviated. Further to this, a likely scenario is that the material exists in the form of a disk wind rather than discrete clouds (e.g., Sim et al. 2008; Schurch & Done 2008), in that case the argument about probability is not relevant and the observation of two partial absorbers reveals the clumpy nature of the wind. In any case, some of the unabsorbed flux may be scattered emission, the 3% residual unabsorbed flux observed in our interpretation of the low-state *XMM* data (Section 3.3) seems likely to be such (allowing for this, of course, increases the inferred cloud covering fraction).

Here, the distance of the absorbers can be estimated from the definition of $\xi$ used in XSTAR, $\xi = \frac{L}{r^2 n}$, where $L$ is the ionizing luminosity integrated from 1 to 1000 Ry, $n$ is the proton density, and $r$ the distance of the material from the central black hole (Tarter et al. 1969). We took the column, ionization, and implied intrinsic luminosity from fits assuming gas densities $n = 10^{10}$ cm$^{-3}$ and $n = 10^{12}$ cm$^{-3}$ to obtain a range of radial estimates for the Compton-thick region $r_{CT} = 5 \times 10^{16}$ to $2 \times 10^{17}$ cm. Both the scaling relations of Kaspi et al. (2000) and Bentz et al. (2006) yield an estimate $r_{BLR} \sim 2 \times 10^{17}$ cm for the radius of the BLR using the 5100 Å flux from Guainazzi et al. (1998). Based on this, the Compton-thick partial-covering absorber appears to lie within the BLR.

1H 0419−577 provides one of few clear examples to date of a Compton-thick partial-covering absorber. PDS 456 exhibits a similar hard excess (at the $3\sigma$ level) in *Suzaku* data to that seen here (Reeves et al. 2009). *RXTE* data for PDS 456 support the *Suzaku* result, showing a very deep Fe K edge from gas of column density ∼$5 \times 10^{23}$ cm$^{-2}$, $\log \xi \sim 2.5$ flowing outward at 50,000 km s$^{-1}$ (Reeves et al. 2002, 2003). The question of gas velocity is interesting, high-velocity outflows in the range 0.1–0.2$c$ (Reeves et al. 2008) have been reported in X-ray data for a number of high-luminosity AGN (e.g., Reeves et al. 2002; Pounds et al. 2003; Dadina & Cappi 2004; Dadina et al. 2005; Chartas et al. 2003) and we suggest that 1H 0419−577 has a high-velocity outflow whose absorption features have yet to be isolated.

Interestingly, model fits to *BeppoSAX* data showed 1H 0419−577 to have a flat component in the hard X-ray regime (modeled in that case as a $\Gamma \sim 1.5$ power law; Guainazzi
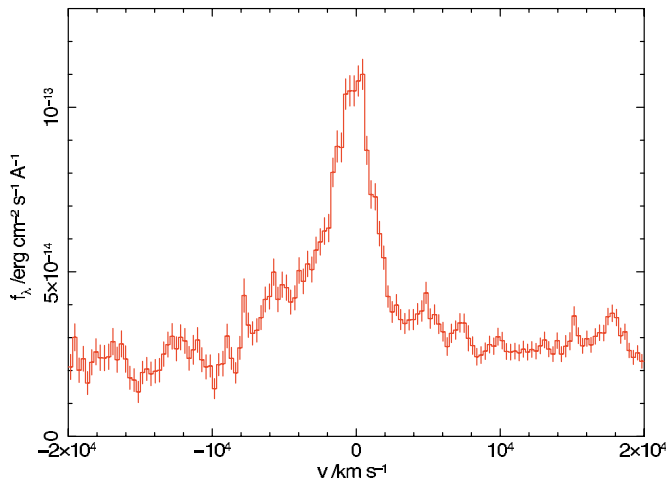
**Figure 4.** *IUE* spectrum of 1H 0419−577 showing the asymmetric C IV profile. (A color version of this figure is available in the online journal.)

et al. 1998), although the hard-band flux is different to that observed by the PIN. If the continuum source is intrinsically constant, then the apparent variability in flux over 15–136 keV can be achieved only if there exists a component of material with $N_H > 10^{25}$ cm$^{-2}$ along the line of sight: the implication of such an extension to high column is not surprising given the establishment of clumps of material in the regime $N_H \sim \times 10^{24}$ cm$^{-2}$ found here.

### 4.2. An Origin for the Absorption in a Disk Wind Associated with the BLR

Unfortunately, the *Suzaku* data for 1H 0419−577 yield little insight into the kinematics of the X-ray absorbers. However, examination of the UV spectra has proved interesting in this regard. Dunn et al. (2007) show the O VI and Lyβ absorption lines to have kinematic components tracing outflow at 200, 100, and 20 km s$^{-1}$, with evidence that the lowest velocity component of gas does not fully cover the source. An *IUE* spectrum of 1H 0419−577 (Figure 4) shows a C IV emission line with an apparent blue wing. This phenomenon is commonly observed in the high-ionization lines in quasar spectra and generally attributed to a lack of flux on the red side of the emission line (Richards et al. 2002; Murray & Chiang 1998). In models where the high-ionization UV emission lines are thought to arise from clouds comprising a disk wind, this profile may be indicative of a disk viewed close to edge-on, such that the observer is looking down the flow of the wind (e.g., Murray & Chiang 1998; Richards et al. 2002). In the case of 1H 0419−577, the C IV profile has a velocity width ∼5000 km s$^{-1}$ (Figure 4) which is consistent with the widths of the O VII and O VIII lines of 7000 ± 3000 km s$^{-1}$ detected by Pounds et al. (2004b). The width of the Fe Kα emission, $\sim 7000^{+9000}_{-7000}$ km s$^{-1}$, detected here is consistent with the UV and soft X-ray results, indicating all these signatures arise in kinematically associated flows. Baskin & Laor (2005) suggest that high $\frac{L}{L_{Edd}}$ is a necessary (but not sufficient) condition for generating a blueshifted C IV profile. The mass of the central black hole in this source has been estimated at $1.3 \times 10^8$ $M_\odot$ (Pounds et al 2004b); taking $L_{bol} \sim (7\text{–}11) \times 10^{46}$ erg s$^{-1}$ we estimate that 1H 0419−577 is operating at $L \sim (3\text{–}6) \times L_{Edd}$. Of particular interest is the prediction of Compton-thick, clumpy, continuum-driven disk winds for Eddington-limited AGN (King & Pounds 2003); this

suggests that similar "hard excesses" will be found for other super-Eddington AGN.

### 4.3. The Bolometric Luminosity of 1H 0419–577

In the optical regime, 1H 0419−577 has observed line strength (Guainazzi et al. 1998) $F_{H\alpha} = 1.6 \times 10^{-12}$ erg cm$^{-2}$ s$^{-1}$ (broad component) with corresponding luminosity $L_{H\alpha} = 3.8 \times 10^{43}$ erg s$^{-1}$. The correlation established between the luminosity of Hα and $L_x$ (Ho et al. 2001; Ward et al. 1988) allows us to estimate the line expected for gas exposed to a given luminosity. Taking the estimate of intrinsic (scattering corrected) 2–10 keV luminosity from our partial-covering model, $L_{2-10} = (2\text{–}3) \times 10^{45}$ erg s$^{-1}$ and the known line-luminosity correlation, we would predict $L_{H\alpha} \sim (0.2\text{–}2) \times 10^{44}$ erg s$^{-1}$ and so the observed Hα line luminosity is consistent with the expected value. The observed O III λ5007 line luminosity is $L_{O III} = 1.4 \times 10^{43}$ erg s$^{-1}$ (Grupe et al. 1999). Meléndez et al. (2008) find a relationship between O III and X-ray luminosities that yields an expected O III luminosity $L_{O III} = (0.8\text{–}3) \times 10^{43}$ erg s$^{-1}$, consistent with that observed. These good agreements between expected and observed line fluxes suggest that our derivation of intrinsic continuum luminosity is reasonable, supporting our application of the absorption and scattering corrections utilized in regard to the source flux.

### 4.4. Fluorescent Line Emission from the Absorbing Zones

The absorbing gas is, naturally, expected to produce fluorescent line emission. The line intensity may depend on a number of factors, the most obvious being the fraction of the source continuum that is intercepted by the absorber. This line could be significant from the Compton-thick layer of gas. We should also distinguish between two cases, one where the fluorescent emission experiences resonant scattering and one where it does not.

Considering Fe Kα emission: at the value of $\xi$ inferred from the fits in Section 3.2, $0.5 \lesssim \log\xi \lesssim 2$, for photon index $\Gamma = 2.3$, we do not expect there to be a significant ion population more highly ionized than Fe XVII (Kallman et al. 2004) and, in this case, this line would not experience substantial resonant scattering. We can then infer approximately the expected line luminosity by multiplying the emission from the spherically symmetric XSTAR absorber model by some filling factor.

The predicted model flux in the Fe Kα line is $L_{Fe} \sim 3^{+3}_{-1} \times 10^{43}$ erg cm$^{-2}$ s$^{-1}$ and the observed luminosity is $\sim 5^{+5}_{-1.5}$% of that predicted for a full shell of gas. Assuming that the disk extends beyond the radius where the gas exists (applicable to the disk wind scenario) then the optically thick disk will hide half of the emission from view (thus the true global covering for the gas is $\sim 10^{+10}_{-3}$% and we denote this $G_f = 0.1$). In the case where the absorber is a smooth equatorial wind seen edge-on, we thus estimate a disk opening angle $\theta \simeq \sin^{-1} G_f \simeq 12^{\circ +12}_{-4}$ (e.g., Pounds & Reeves 2008, who found $G_f \sim 0.3$ for PG1211+143).

How reasonable is such a wind opening angle? If we had surveyed a sample of AGN which had been selected in a way independent of orientation, we would expect to be viewing about 10% of them through the equatorial wind. Such an unbiased sample has not been investigated from this perspective, but this probability of occurrence implies that the inferred source orientation of 1H 0419–0577 is not particularly surprising.

However, given the uncertainty in the ionization of the Compton-thick zone, and given the simplicity of the model adopted, we cannot exclude the possibility that this zone has

log $\xi \gtrsim 2.5$, in which case charged states more highly ionized than Fe xviii should be populated and Fe K$\alpha$ is expected to suffer resonant scattering. Resonant scattering will significantly deplete the emitted line photons, by the Auger effect (for Li- to F-like states) and by photoelectric absorption, on repeated scatterings (as discussed by, e.g., Turner & Miller 2009).

In this case, the geometry of the absorber and its orientation with respect to the observer play an even more key role than in the nonresonant case (e.g., Ferland et al. 1992): most line photons will be scattered and escape through the upper and lower surfaces of the disk. If we are viewing the disk edge-on, most of those photons will be lost from the line of sight. Hence, in the resonant scattering case, extremely large line suppression factors are possible, in which case the estimated filling factor deduced assuming no resonant scattering is very much a lower limit to the true filling factor.

## 5. CONCLUSIONS

A marked "hard excess" of counts is detected in the *Suzaku* PIN data for 1H 0419−577 relative to the predicted flux based on fits below 10 keV. The *Suzaku* data can be fitted using an absorption-dominated model showing that Compton-thick partial-covering X-ray absorbers exist in the type 1 AGN, 1H 0419−577 and probably other AGN. The data are consistent with a clumpy disk wind that provides the X-ray absorption from gas residing at radii inside of the BLR. The observed Fe K$\alpha$ line emission is consistent with an origin in an equatorial disk wind and the widths of measured soft X-ray and UV emission lines support this picture. We find that blurred reflection models cannot satisfactorily fit the source and so the 1H 0419−577 data provide a rare distinction between two observationally similar classes of model.

## REFERENCES

Baskin, A., & Laor, A. 2005, MNRAS, 356, 1029
Bentz, M. C., Peterson, B. M., Pogge, R. W., Vestergaard, M., & Onken, C. A. 2006, ApJ, 644, 133
Boldt, E., & Leiter, D. 1987, ApJ, 322, L1
Braito, V., et al. 2007, ApJ, 670, 978
Chartas, G., Brandt, W. N., & Gallagher, S. C. 2003, ApJ, 595, 85
Dadina, M., & Cappi, M. 2004, A&A, 413, 921
Dadina, M., Cappi, M., Malaguti, G., Ponti, G., & de Rosa, A. 2005, A&A, 442, 461
Deluit, S., & Courvoisier, T. J.-L. 2003, A&A, 399, 77
Dunn, J. P., Crenshaw, D. M., Kraemer, S. B., & Gabel, J. R. 2007, AJ, 134, 1061
Elvis, M., et al. 1994, ApJS, 95, 1
Fabian, A. C., Miniutti, G., Iwasawa, K., & Ross, R. R. 2005, MNRAS, 361, 795

Ferland, G. J., Peterson, B. M., Horne, K., Welsh, W. F., & Nahar, S. N. 1992, ApJ, 387, 95
George, I. M., & Fabian, A. C. 1991, MNRAS, 249, 352
Gruber, D. E., Matteson, J. L., Peterson, L. E., & Jung, G. V. 1999, ApJ, 520, 124
Grupe, D. 1996, PhD thesis, Univ. Göttingen
Grupe, D., Beuermann, K., Mannheim, K., & Thomas, H.-C. 1999, A&A, 350, 805
Guainazzi, M., et al. 1998, A&A, 339, 327
Ho, L. C., et al. 2001, ApJ, 549, L51
Holt, S. S., Mushotzky, R. F., Boldt, E. A., Serlemitsos, P. J., Becker, R. H., Szymkowiak, A. E., & White, N. E. 1980, ApJ, 241, L13
Inoue, H., & Matsumoto, C. 2003, PASJ, 55, 625
Kallman, T. R., Palmeri, P., Bautista, M. A., Mendoza, C., & Krolik, J. H. 2004, ApJS, 155, 675
Kaspi, S., Smith, P. S., Netzer, H., Maoz, D., Jannuzi, B. T., & Giveon, U. 2000, ApJ, 533, 631
King, A. R., & Pounds, K. A. 2003, MNRAS, 345, 657
Koyama, K., et al. 2007, PASJ, 59, 23
Kraemer, S. B., et al. 2005, ApJ, 633, 693
Laor, A. 1991, ApJ, 376, 90
Marshall, H. L., Fruscione, A., & Carone, T. E. 1995, ApJ, 439, 90
McKernan, B., & Yaqoob, T. 1998, ApJ, 501, L29
Meléndez, M., et al. 2008, ApJ, 682, 94
Miller, L., Turner, T. J., & Reeves, J. N. 2008, A&A, 483, 437
Miller, L., Turner, T. J., Reeves, J. N., George, I. M., Kraemer, S. B., & Wingert, B. 2007, A&A, 463, 131
Miniutti, G., & Fabian, A. C. 2004, MNRAS, 349, 1435
Miniutti, G., Fabian, A. C., Goyder, R., & Lasenby, A. N. 2003, MNRAS, 344, L22
Miniutti, G., et al. 2007, PASJ, 59, 315
Mitsuda, K., et al. 2007, PASJ, 59, 1
Murray, N., & Chiang, J. 1998, ApJ, 494, 125
Netzer, H., Chelouche, D., George, I. M., Turner, T. J., Crenshaw, D. M., Kraemer, S. B., & Nandra, K. 2002, ApJ, 571, 256
Page, K. L., Pounds, K. A., Reeves, J. N., & O'Brien, P. T. 2002, MNRAS, 330, L1
Papadakis, I. E., Petrucci, P. O., Maraschi, L., McHardy, I. M., Uttley, P., & Haardt, F. 2002, ApJ, 573, 92
Piro, L., Yamauchi, M., & Matsuoka, M. 1992, Nuovo Cimento C, 15, 811
Pounds, K. A., & Reeves, J. N. 2008, arXiv:0811.3108
Pounds, K. A., Reeves, J. N., King, A. R., Page, K. L., O'Brien, P. T., & Turner, M. J. L. 2003, MNRAS, 345, 705
Pounds, K. A., Reeves, J. N., Page, K. L., & O'Brien, P. T. 2004a, ApJ, 605, 670
Pounds, K. A., Reeves, J. N., Page, K. L., & O'Brien, P. T. 2004b, ApJ, 616, 696
Reeves, J., Done, C., Pounds, K., Terashima, Y., Hayashida, K., Anabuki, N., Uchino, M., & Turner, M. 2008, MNRAS, 385, L108
Reeves, J. N., O'Brien, P. T., & Ward, M. J. 2003, ApJ, 593, L65
Reeves, J. N., et al. 2009, ApJ, submitted
Reeves, J. N., Wynn, G., O'Brien, P. T., & Pounds, K. A. 2002, MNRAS, 336, L56
Reichert, G. A., Mushotzky, R. F., Holt, S. S., & Petre, R. 1985, ApJ, 296, 69
Richards, G. T., Vanden Berk, D. E., Reichard, T. A., Hall, P. B., Schneider, D. P., SubbaRao, M., Thakar, A. R., & York, D. G. 2002, AJ, 124, 1
Risaliti, G., Bianchi, S., Matt, G., Baldi, A., Elvis, M., Fabbiano, G., & Zezas, A. 2005, ApJ, 630, L129
Ross, R. R., & Fabian, A. C. 2005, MNRAS, 358, 211
Schurch, N. J., & Done, C. 2008, MNRAS, 386, L1
Sim, S. A., Long, K. S., Miller, L., & Turner, T. J. 2008, MNRAS, 388, 611
Takahashi, T., et al. 2007, PASJ, 59, 35
Tarter, C. B., Tucker, W. H., & Salpeter, E. E. 1969, ApJ, 156, 943
Thomas, H.-C., Beuermann, K., Reinsch, K., Schwope, A. D., Truemper, J., & Voges, W. 1998, A&A, 335, 467
Tueller, J., Mushotzky, R. F., Barthelmy, S., Cannizzo, J. K., Gehrels, N., Markwardt, C. B., Skinner, G. K., & Winter, L. M. 2008, ApJ, 681, 113
Turner, T. J., & Miller, L. 2009, A&A Rev., 17, 47
Turner, T. J., Miller, L., Reeves, J. N., & Kraemer, S. B. 2007, A&A, 475, 121
Turner, T. J., Reeves, J. N., Kraemer, S. B., & Miller, L. 2008, A&A, 483, 161
Turner, T. J., et al. 1999, ApJ, 510, 178
Vaughan, S., & Fabian, A. C. 2004, MNRAS, 348, 1415
Ward, M. J., Done, C., Fabian, A. C., Tennant, A. F., & Shafer, R. A. 1988, ApJ, 324, 767
Young, A. J., Lee, J. C., Fabian, A. C., Reynolds, C. S., Gibson, R. R., & Canizares, C. R. 2005, ApJ, 631, 733